Carbonate U-Pb Ages Constrain Paleocene Motion Along the Altyn Tagh Fault in Response to the India-Asia Collision

Kexin Yi, Feng Cheng, Marc Jolivet, Jiaming Li, Zhaojie Guo

Geophysical Research Letters

RESEARCH LETTER
10.1029/2023GL107716

Carbonate U-Pb Ages Constrain Paleocene Motion Along the Altyn Tagh Fault in Response to the India-Asia Collision

Kexin Yi[1], Feng Cheng[1], Marc Jolivet[2], Jiaming Li[1], and Zhaojie Guo[1]

[1]Key Laboratory of Orogenic Belts and Crustal Evolution, School of Earth and Space Sciences, Peking University, Beijing, China, [2]Géosciences Rennes–UMR CNRS 6118, Université de Rennes, Rennes, France

Key Points:

- Calcite U-Pb dating yields ca. 59 Ma age for carbonate strata in the East Xorkol Basin
- Xorkol Basin was a pull-apart basin during the Paleocene due to the left-lateral strike-slip faulting along the Altyn Tagh fault
- Widespread Paleocene-Eocene tectonism in Northern Tibet highlights the far-field effect of the India-Asia collision

Supporting Information:

Supporting Information may be found in the online version of this article.

Correspondence to:

F. Cheng and Z. Guo,
cfcf.chengfeng@gmail.com;
zjguo@pku.edu.cn

Citation:

Yi, K., Cheng, F., Jolivet, M., Li, J., & Guo, Z. (2024). Carbonate U-Pb ages constrain Paleocene motion along the Altyn Tagh fault in response to the India-Asia collision. *Geophysical Research Letters*, *51*, e2023GL107716. https://doi.org/10.1029/2023GL107716

Received 6 DEC 2023
Accepted 26 FEB 2024

Author Contributions:

Conceptualization: Feng Cheng, Zhaojie Guo
Data curation: Kexin Yi
Formal analysis: Feng Cheng
Funding acquisition: Zhaojie Guo
Investigation: Kexin Yi, Feng Cheng, Jiaming Li, Zhaojie Guo
Methodology: Kexin Yi, Zhaojie Guo
Project administration: Zhaojie Guo
Resources: Zhaojie Guo
Supervision: Feng Cheng, Marc Jolivet, Zhaojie Guo
Validation: Kexin Yi, Feng Cheng, Jiaming Li, Zhaojie Guo
Writing – original draft: Kexin Yi
Writing – review & editing: Feng Cheng, Marc Jolivet, Jiaming Li, Zhaojie Guo

Abstract The kinematics and deformation pattern along the Altyn Tagh fault (ATF), one of the largest strike-slip faults on Earth is of great significance for understanding the growth of the Tibetan Plateau. However, the initial rupture along the ATF remains debated given the limited constraints on the depositional age of associated Cenozoic syntectonic strata. Here we investigated the syntectonic Cenozoic strata in the Xorkol Basin, associated with the strike-slip faulting along the ATF. New uranium-lead analyses of the carbonate deposits in the Paleogene strata yield dates of 58.9 ± 1.29 Ma, representing the initial rupture of the ATF. This first documented radioisotopic age coincides with the ca. 60 Ma onset timing of India-Asia collision, highlighting its far-field effect at the northern edge of the Tibetan Plateau. We infer that the deformation of the entire Tibetan Plateau started synchronously with the India-Asia collision.

Plain Language Summary Carbonate U-Pb dating techniques applied to rocks associated with the Altyn Tagh fault, a major fault in North Tibet, reveal that the fault started slipping about 58.9 million years ago, coinciding with the time when India collided with Asia. This finding provides new constraints on when and where this fault formed and suggests that the northern Tibetan Plateau started deformation earlier than previously thought. This result emphasizes that the entire Tibetan Plateau deformed simultaneously in the early Cenozoic.

1. Introduction

The formation of the Tibetan Plateau as a result of the Cenozoic India-Asia collision had a profound impact on the Asian tectonics configuration and climate dynamics (e.g., An et al., 2001; Ding et al., 2022). However, the geodynamic mechanisms that built the plateau remain disputed. Two main end-member models have been proposed: (a) The Tibetan Plateau has grown progressively and the northward-propagating deformation reached its present-day northeastern edge no earlier than the Neogene (e.g., England & Houseman, 1985; Tapponnier et al., 2001); (b) The northern and southern Tibetan Plateau underwent Paleogene deformation related to the incipient India-Asia collision (e.g., Dupont-Nivet et al., 2004; Jolivet et al., 2001; Yin et al., 2002). Determining the onset timing of Cenozoic deformation along the tectonic structures in the northern Tibetan Plateau is critical in resolving this dispute, as it will provide insights into how the northern Tibetan Plateau responded to the collision.

The Altyn Tagh fault (ATF) is a lithospheric left-lateral strike-slip fault that marks the northwestern boundary of the Tibetan Plateau (Yin et al., 2002) (Figure 1). Despite a great achievement on the timing of deformation in the northern Tibetan Plateau, the initiation age and configuration of the ATF remain debated given its long-lasting growth history. Yin et al. (2002) proposed a ca. 49 Ma initiation of strike-slip faulting along the present ATF based on field investigation, magnetostratigraphy and subsurface reflection data. However, others have proposed different initiation timing and configurations. For instance, Tapponnier et al. (2001) proposed that the ATF gradually propagated from west to east during the Cenozoic. Yue and Liou (1999) proposed an early Oligocene initiation of strike-slip activity by analyzing the sedimentary basins along the fault. Inspired by the strike-slip duplex model raised by Cowgill et al. (2000), L. Wu et al. (2019) proposed that the ATF fault system initiated at ca. 53.5 Ma, featured by a large restraining bend consisting of the North Altyn fault and Jinyanshan fault, with the central ATF forming in the Miocene.

By far, low-temperature thermochronology on basement rocks that outcrop along the ATF is widely used to date the initial rupture along the ATF. However, the limited exhumation generated by strike-slip motion makes it challenging to capture the initiation of such motion through recorded ages. In addition, some published data are based on single-sample inverse thermal history modeling (e.g., Qi et al., 2016; Shi et al., 2018), the resilience and

10.1029/2023GL107716

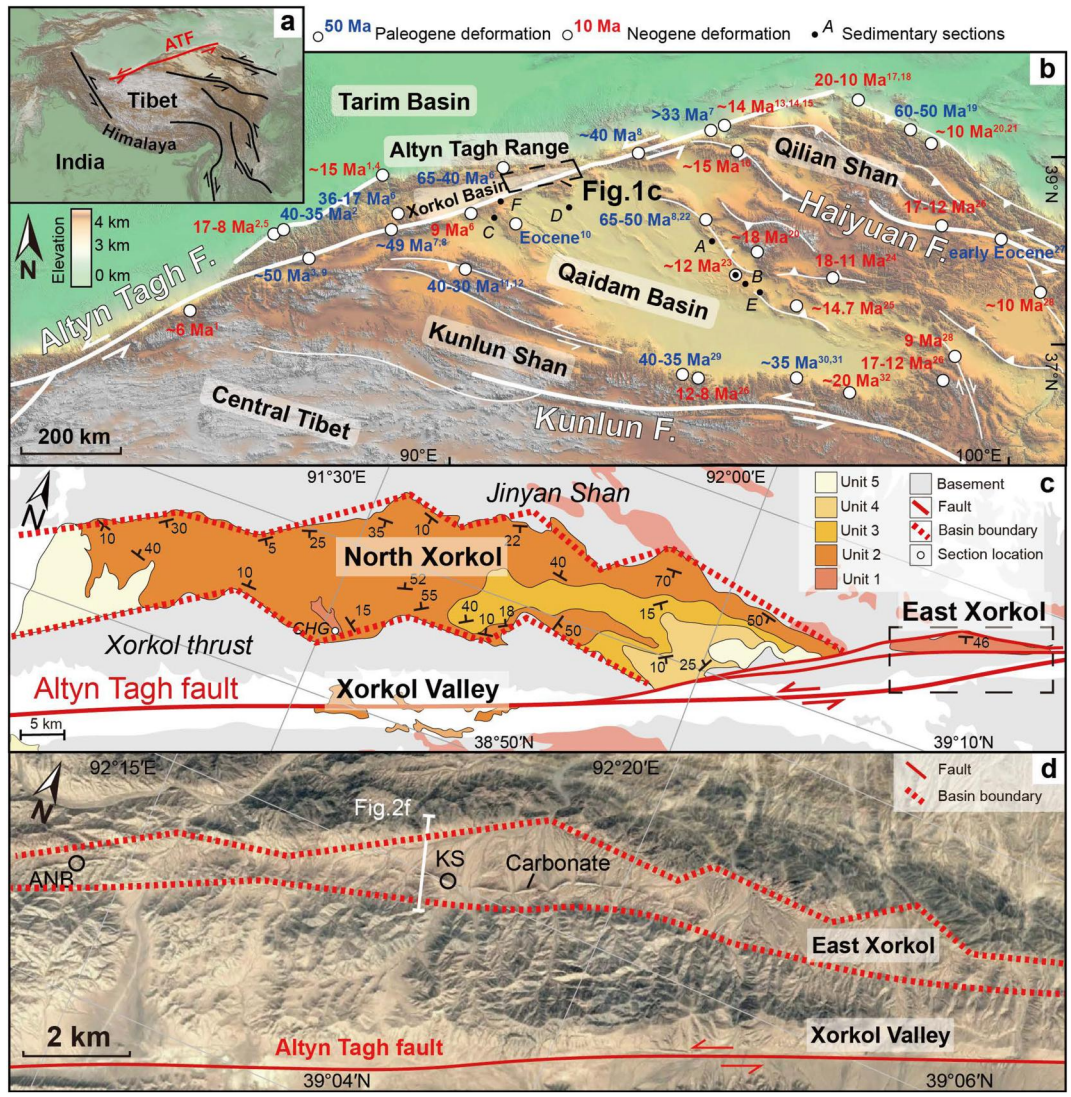

Figure 1. Maps of the study area. (a) Tectonic location of Altyn Tagh fault defining the northern boundary of the Tibetan Plateau. Major strike-slip faults are shown in black lines. (b) SRTM-based digital topographic map of the northern Tibetan Plateau and the study area with distribution of the major timing of deformation. References are shown in Table S1 of Supporting Information S1. Locations of sedimentary sections in Figure 5 are denoted. (c) Simplified geological map of the North and East Xorkol basins modified from XBGMR (1981) and QBGMR (1986). Unit 1–5 are lithostratigraphic units corresponding to Paleogene-Eocene, Oligocene, lower Miocene, upper Miocene, and Quaternary strata respectively. CHG: Caihonggou section. (d) Google Earth satellite image of East Xorkol Basin with sampling locations. Note the serrated basin boundary and carbonate rock strata. The location of the geological profile in Figure 2f is indicated.

soundness of which remain questionable (Green & Duddy, 2021). Therefore, the exhumation history of the basement rocks along the ATF remains elusive, highlighting the need for a comprehensive understanding that integrates various methods.

Cenozoic syntectonic strata are well-developed along the northern and southern sides of the ATF. These terrestrial strata are associated with the ATF, providing a direct proxy to address the kinematics and timing of faulting. However, due to the lack of tephra layers and index fossils, the exact depositional age of these strata remains poorly constrained. Recent advancements in calcite U-Pb dating offer a promising tool to establish the absolute depositional age of the carbonate strata (e.g., Parrish et al., 2019; Rembe et al., 2022; Roberts et al., 2020). Here we report the first U-Pb radioisotopic age of lacustrine carbonates in the syntectonic strata that outcrop along the ATF. The obtained age of ca. 60 Ma suggests that the Cenozoic strike-slip motion along the ATF initiated during

the Paleocene, highlighting the synchronous deformation at both the northern and southern margins of the Tibetan Plateau in the early Cenozoic.

2. Methods

Field investigations were conducted in the East Xorkol Basin. The Xorkol Basin is an intermontane basin within the Altyn Tagh Range. Previous studies have reached an agreement that the formation of the Xorkol Basin has been governed by the ATF. Evidence includes the narrow and elongated geometry, the finer-grained deposits in the center compared to the edges, a series of stepped faults at the boundaries, and the presence of syntectonic conglomerates along the boundaries (e.g., Z. L. Chen et al., 2004; E. Wang et al., 2008).

The Xorkol Basin is subdivided into three parts: the Xorkol Valley Basin covered by Quaternary deposits, the North Xorkol Basin which accumulates Paleogene-Neogene sediments, and the eastern end named East Xorkol Basin (Figure 1b). The bedrock surrounding the East Xorkol Basin is attributed to the Ordovician Lapeiquan Group, which is composed of basaltic-andesitic volcanic rocks, slightly-metamorphosed clastic rocks, and carbonate rocks (QBGMR, 1986). Recent studies assigned a meso-Proterozoic depositional age on these carbonate rocks based on detailed mapping and structural analysis (e.g., B. Chen, 2018).

A total of 25 carbonate samples were collected from these Cenozoic strata, and 19 carbonate thick sections were dated using laser ablation-inductively coupled plasma-mass spectrometry (LA-ICP-MS) at the State Key Laboratory of Lithospheric Evolution, Institute of Geology and Geophysics, Chinese Academy of Sciences, Beijing. We followed the analytical and data processing routine described by S. T. Wu et al. (2022). Specific details of sampling, sample preparation, and dating are given in Text S1 of Supporting Information S1. A total of 40 laser ablation spots were analyzed for each sample. Calcite veins, probably indicating late fluid circulations, were avoided during analysis to minimize potential contamination.

3. Results and Discussion

3.1. The Syntectonic Strata in the East Xorkol Basin

Here we provide additional evidence demonstrating that the North and East Xorkol basins are pull-apart basins of the strike-slip ATF. First, satellite images show that the both North and East Xorkol basins are characterized by serrated boundaries and rhomb grabens (Figures 1c and 1d); distinct topographic features resulting from the evolution of a pull-apart basin (Aydin & Nur, 1982). Second, the Paleogene strata in the East Xorkol Basin exhibit typical syntectonic features associated with the strike-slip faulting in a pull-apart basin (Christie-Blick & Biddle, 1985), as characterized by the following observations. The strata in the basin consist of brownish conglomerates along the margins and the carbonate rocks are interlayered with reddish mudstone and greenish sandstone at the center (Figure 2; Figures S1a and S1b in Supporting Information S1). The strata are in fault contact with the bedrock on both the northern and southern sides of the basin, evidenced by brecciated sediments series and fault gouges (Figures 2b, 2c, and 2e). Along the northern boundary, brecciated conglomerates display the tectonic cleavage that strongly imprints the original bedding (Figure 2c). Fault scarps and fault gouges with a strike of approximately N80° were also observed between the strata and the bedrock. Slickensides on the fault surface indicated a left-lateral strike-slip movement compatible with that of the ATF (Figure S1c in Supporting Information S1). The evolution of the depositional environment from alluvial fan to lacustrine carbonate deposits, coarse lateral sediment inputs, as well as the mirror-like symmetry on both the northern and southern sides of the basin, indicates syn-strike-slip fault sedimentation in the East Xorkol basin along the ATF.

Therefore, we suggest that the onset of Cenozoic sedimentation in the North and East Xorkol basins was associated with the initial tectonic activities of the ATF, and the initial depositional age of strata within the basin should be coincident with the initiation of strike-slip faulting along the ATF. The carbonate crops are either adjacent to or interbedded with the clastic rocks (Figure S1 in Supporting Information S1), indicating that the depositional age of the carbonate rocks might be slightly younger than the initial sedimentation of the strata. It is worth noting that the timing of deposition of these strata is coincident with the onset of basin formation. This precluded the possibility of these strata being basement rocks that were re-exposed due to the rejuvenated fault activities. This inference is further evidenced by the distinct contrast between the basin's strata and the surrounding basement rock, which contains gray phyllite and light gray dolomite.

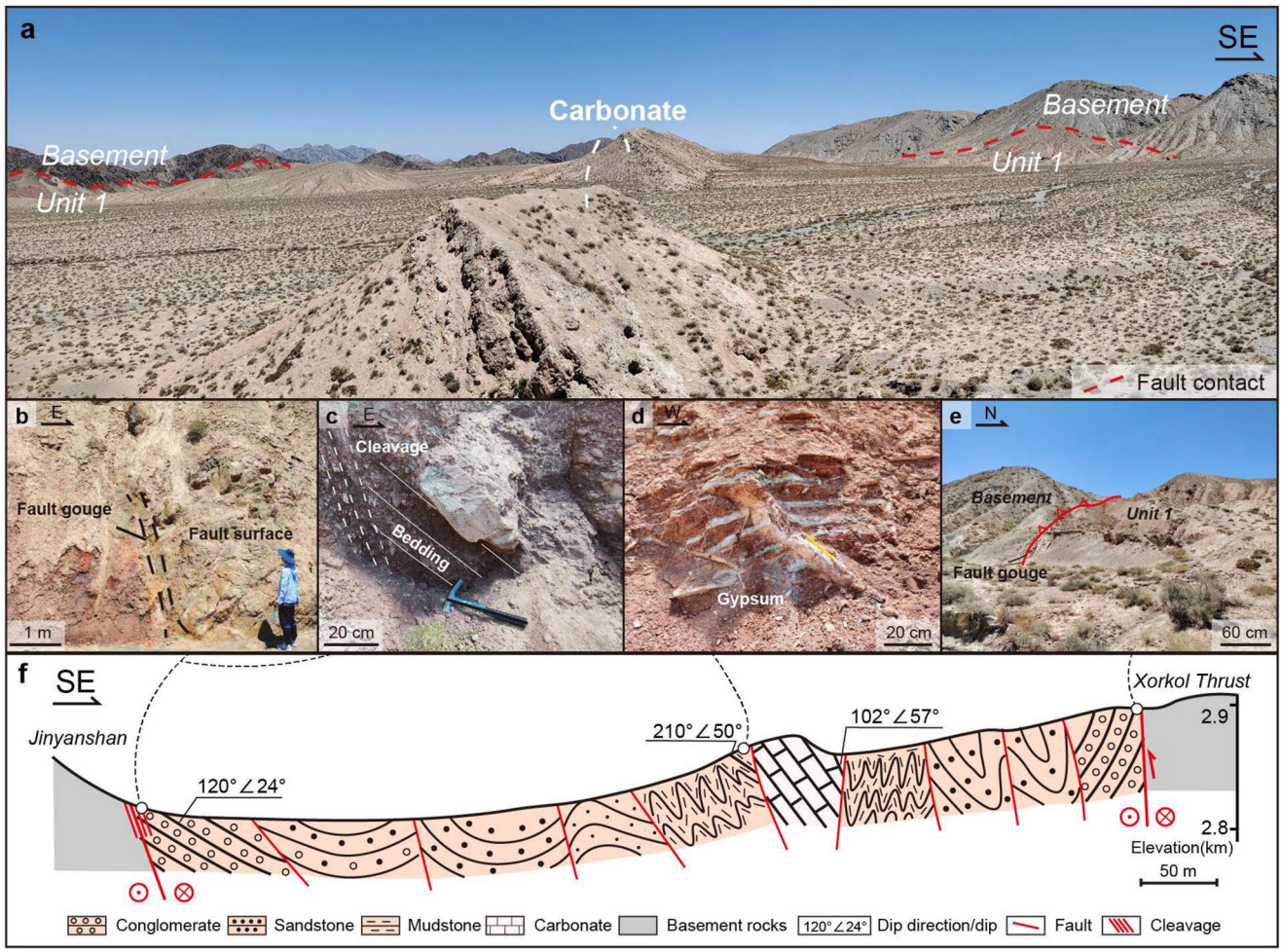

Figure 2. Field features of the East Xorkol Basin. (a) Panoramic photograph of the East Xorkol Basin. (b) Strike-slip fault surface with fault gouge and slickensides at the northern boundary of the basin. (c) Outcropped brecciated conglomerates within which a strong imprint of the tectonic cleavage replaces the original bedding. (d) Deformed fine-grained strata in the East Xorkol Basin. (e) Thrust fault with fault gouge at the basin's southern boundary. (f) Geological profile of the East Xorkol Basin.

3.2. Carbonate U-Pb Dating of Syntectonic Strata

The exposed carbonate outcrops in the Cenozoic strata in the East Xorkol Basin are about 60 cm thick at the ANB site and about 30 m thick at the KS site (Figures 3a and 3b). They are exposed with bedding parallel to the long axis of the basin. The carbonate is relatively homogeneous in appearance and exhibits a white and pink mottled coloration. It has been partially broken, most probably by tectonic activity, with tilted sedimentary layers that are not always clearly visible. The deposits are mainly characterized by primary micritic limestone displaying small-scale microbialite features. Evidence of alteration on hand specimen is scarce and the absence of post-depositional re-crystallization is confirmed by cathodoluminescence (CL) analysis (especially marked by evenly colored micrite) (Figure 3). This feature further affirms that the carbonate belongs to the Cenozoic syntectonic strata instead of the bedrock. Additional sample photos can be found in Figure S1 of Supporting Information S1.

We collected a total of 19 carbonate samples from two outcrops for U-Pb dating, of which 11 yielded coherent ages (Table S2 in Supporting Information S1). The complete data is available in Data Set S1, and the Tera-Wasserburg plots for each sample are present in Figure S2 of Supporting Information S1. These ages span from 43.0 Ma to 76.6 Ma. This relatively large uncertainty might be attributed to high common-Pb content in the individual samples. However, the carbonates from these 11 samples display homogeneous features in the microscope and cathodoluminescence images (Figure 3), thus the entire data set obtained from samples defines a single age population.

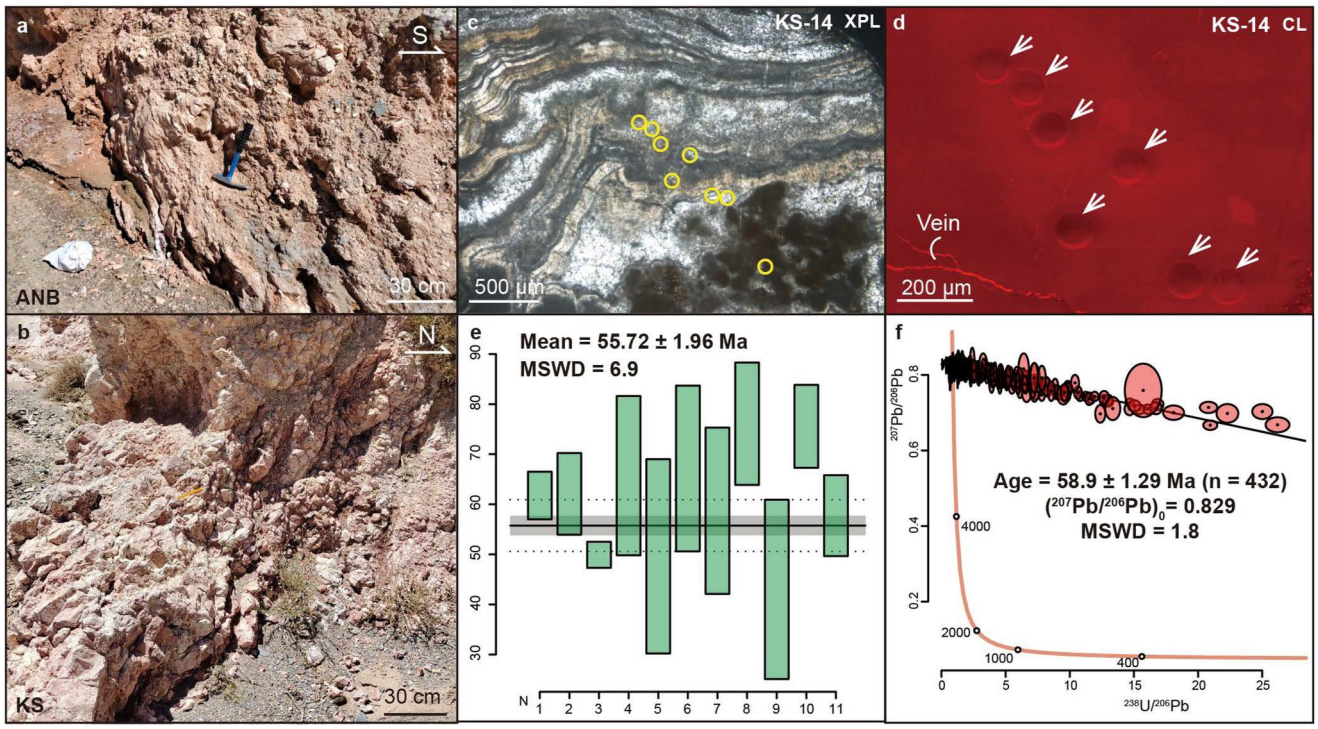

Figure 3. Outcrop, samples, and dating results of carbonate rocks. (a and b) ANB and KS outcrops of carbonate rocks exhibiting fracturing, with a relatively fresh appearance and moderate weathering. (c and d) Photomicrograph and cathodoluminescence (CL) image of sample KS-14, revealing microbial features and primary sedimentary structures as a representative example. The uniformity of color observed in the CL image suggests that the sample has undergone little post-depositional alteration. (e) Weighted mean U-Pb ages of carbonate samples. (f) Tera-Wasserburg plot for the whole 432 data. The red lines are Concordia curves. Ellipses are 95% confidence level.

We calculated two ages to describe the carbonate: a weighted mean age of 55.7 ± 1.96 Ma (based on 11 samples), and a regressed lower intercept age of 58.9 ± 1.29 Ma (based on a total of 432 spot analysis). The regressed age is slightly older than the weighted mean age, which is sensitive to large error margins carried by some of the data. We thus consider the lower intercept U-Pb age of 58.9 ± 1.29 Ma as a robust estimate of the age of the carbonate deposits in the East Xorkol Basin.

3.3. Paleocene Deformation Along the ATF

We report a new radioisotopic time constraint of 58.9 ± 1.29 Ma for the depositional age of carbonate strata in the East Xorkol Basin. This depositional age demonstrates that the sedimentation in the East Xorkol Basin initiated during the late Paleocene. Given the direct correlation between basin formation and ATF deformation, and considering the syntectonic nature of the strata, we propose that the initiation of strike-slip motion along the ATF occurred no later than 58.9 Ma, leading to the formation of the East Xorkol Basin as a composite pull-apart basin (Figure 4).

This result further contributes to our understanding of the initiation timing and configuration of the ATF. First, we provide the first direct dating of syn-tectonic strata along the ATF, yielding the earliest deformation time, slightly predating previous research based on stratigraphy and thermochronology (Cheng et al., 2015, 2016; H. Xie et al., 2022; Yin et al., 2002). Second, we reveal that the initial rupture along the ATF occurred in its central segment of the modern ATF system. This challenges the notion of a gradual northeastward propagation of the ATF (Jiao et al., 2023; Tapponnier et al., 2001) or the proposal that the ATF system initiated at the North Altyn fault (Gao et al., 2022; L. Wu et al., 2019) (Figure 1). Instead, our results show that the modern configuration of the ATF might have already been established since its initial stage in the early Cenozoic.

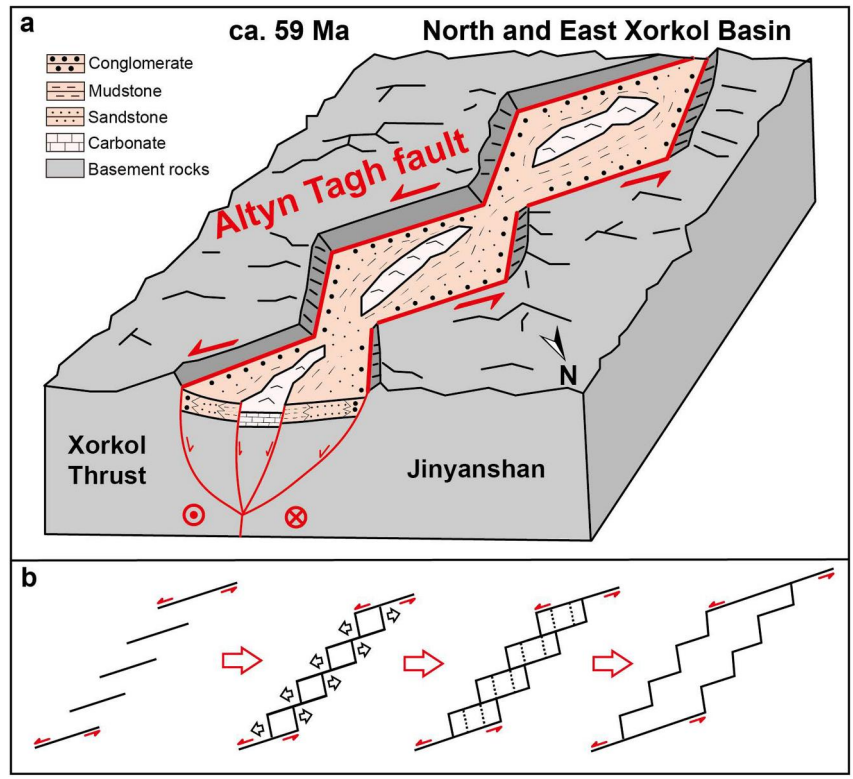

Figure 4. Block diagram illustrating the formation of the North and East Xorkol basins. The left-lateral motion of the Altyn Tagh fault formed en-enchelon, pull-apart basins and led to the early Cenozoic syntectonic sedimentation, no later than 59 Ma. (b) Model showing formation of a composite pull-apart basin associated with en enchelon strike-slip faults, modified after Aydin and Nur (1982). Note that the left-lateral faulting would induce the development of small grabens, then coalescing into composite structures, and finally forming a large basin with a serrated basin boundary.

3.4. Insights on Paleocene-Eocene Strata and Deformation in the Northern Tibetan Plateau

The fine-grained deposits in the East Xorkol Basin exhibit similarities with the red clay layers in the North Xorkol Basin (Figure 5c), whose depositional age has been constrained to >51 Ma by recent magnetostratigraphy studies (Li et al., 2018). Furthermore, the deposits share a similar deposition pattern with the strata in the south of the ATF, including (a) distal fine-grained facies exhibiting massive reddish mudstone interbedded with greenish-gray sandstone that contains high levels of carbonate and gypsum and (b) proximal syntectonic conglomerate facies, mostly composed of poorly sorted matrix-supported pebbles-boulders (e.g., Lu et al., 2019) (Figures 5b and 5g). Therefore, we further suggest that the onset of deposition in the northern Tibetan Plateau is earlier than or equal to ca. 58.9 Ma.

While sedimentation onset has been considered to be closely associated with the initial deformation (e.g., W. Wang et al., 2017; Yin et al., 2002), we suggest that the relief building in the northern Tibetan Plateau initiated in the early Cenozoic. While mountain building in the Neogene, especially Miocene, is better recorded by the low-temperature thermochronology studies, rapid exhumation from Paleocene to Oligocene has also been observed in the Altyn Tagh Range, Qilian Shan and Kunlun Shan (e.g., He et al., 2021; Jolivet et al., 2001; Sobel et al., 2001) (Figure 1b). By comparing the timing of rapid basement exhumation with the onset timing of growth strata, Cheng et al. (2023) further indicates Paleogene tectonic activity in the northern Tibetan Plateau.

The initial continental collision between India and Asia plates is indicated to be 65–60 Ma ago (e.g., Cai et al., 2011; Ding et al., 2022; Hu et al., 2015; Yin & Harrison, 2000). We demonstrate that the deformation of the northern Tibetan Plateau initiated near-simultaneously with the collision. This implies that the collision-originated stress swiftly transferred to the north and instigated the tectonics activity along the ATF and in the northern Tibetan Plateau, even far into the Tian Shan (e.g., Jolivet et al., 2010). Several numerical simulations of

10.1029/2023GL107716

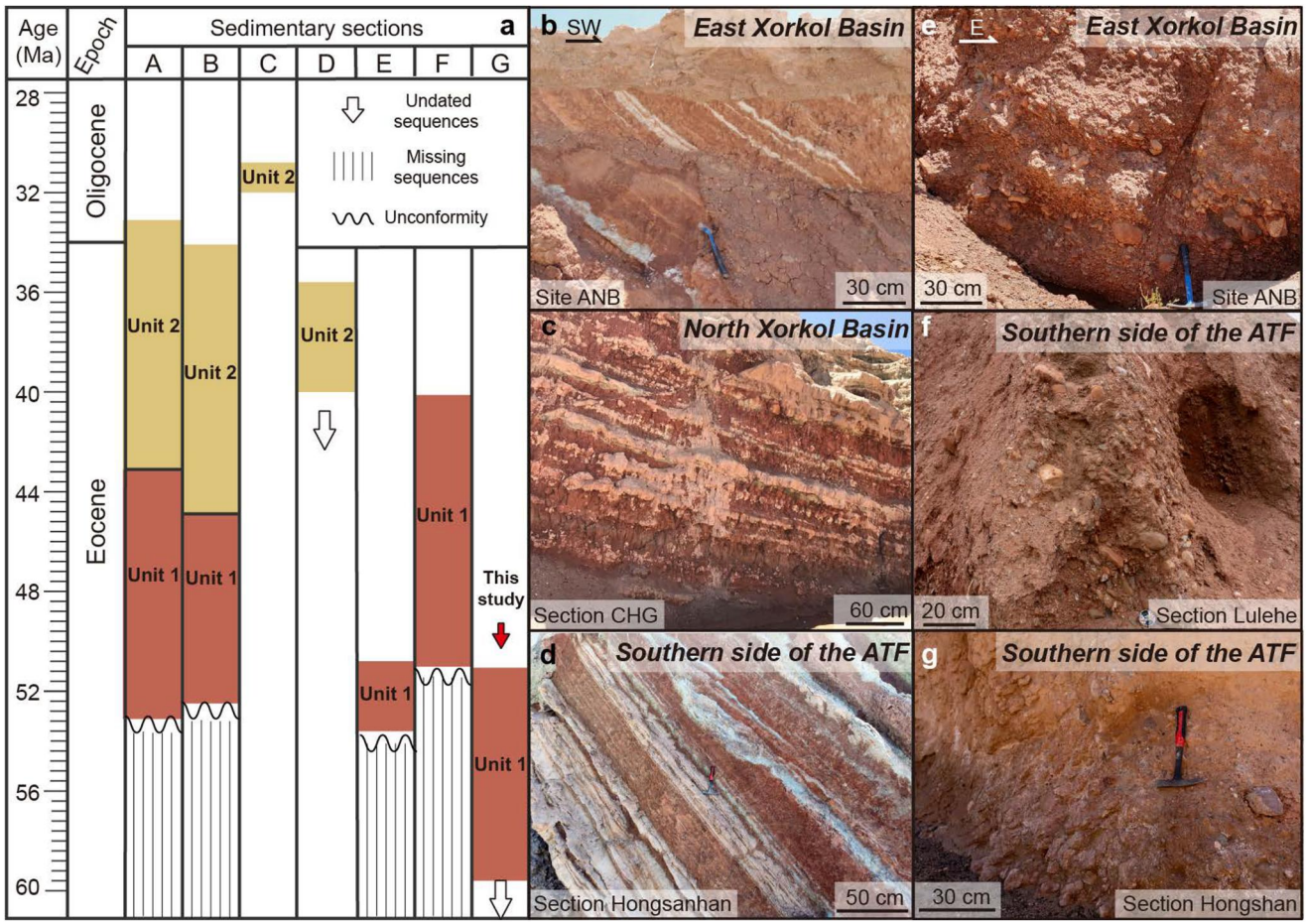

Figure 5. Paleogene strata surrounding the Altyn Tagh fault (ATF). (a) Compiled chronostratigraphic studies of the Paleogene strata Unit 1 and 2, modified from Hu et al. (2022). Section locations are indicated in Figure 1b, and references are supplied in Table S3 of Supporting Information S1. (b) Fine-grained strata in the East Xorkol Basin. (c and d) Fine-grained Unit 1 from the Caihonggou section (section CHG in Figure 1c) in the North Xorkol Basin and the Hongsanhan section (section E in Figure 1b) in the south of the ATF. (e) Syntectonic conglomerate in the East Xorkol Basin. (f and g) Syntectonic conglomerate in Unit 1 from the Lulehe and Hongshan sections (sections A and B in Figure 1b) in the south of the ATF. The strata exhibit similar characteristics across the described sections.

the tectonic growth of the Tibetan Plateau have been established to explain this instant far-field deformation, highlighting the importance of the strong Tarim basement (e.g., Dayem et al., 2009; Xu et al., 2021), the relatively strong Qaidam basement (Cheng et al., 2017; Huangfu et al., 2022; R. Xie et al., 2023), and the lithospheric sutures zones forming pre-existing weaknesses (Cheng et al., 2021; Kelly et al., 2020; Kong et al., 1997; Mouthereau et al., 2013; Zuza et al., 2020) during this process. The contrast in lithospheric strength between the strong Tarim block and the weaker Tibet is a prerequisite for the instant distal orogenesis (Yin & Harrison, 2000). Meanwhile, the Qaidam crust is relatively strong and has the capacity to resist internal deformation (Cheng et al., 2017). Thus, the crustal deformation is concentrated on the pre-existing weaknesses such as sutures and faults, including the ATF (e.g., L. Chen et al., 2017; Cheng et al., 2021).

4. Conclusion

In this study, we provide the first carbonate U-Pb dating, which yields 58.9 ± 1.29 Ma from the syntectonic sediments in the pull apart East Xorkol Basin. This result provides compelling evidence that the ATF initiated its strike-slip motion during the Paleocene-early Eocene. This age estimate is also indicative of the depositional age of the syntectonic strata in the adjacent area, suggesting that the syntectonic sedimentation in the northern Tibetan Plateau initiated during the Paleogene. This result highlights the synchronized onset of deformation of the entire Tibetan Plateau with the initial India-Asia collision.

Data Availability Statement

Supporting information is available at Yi et al. (2023).

Acknowledgments
This paper is dedicated to the memory of Prof. An Yin (1959–2023), an outstanding geologist who devoted his life to Tibetan Plateau research. Financial support for this study was provided by the Key Program of the National Natural Science Foundation of China (Grant 41930213). Yi expresses gratitude for the financial support received from the China Scholarship Council for sponsoring her visit to the Université de Rennes. We gratefully acknowledge the assistance of Haiyan Cao during the fieldwork and Shitou Wu during measurements in the laboratory. We thank Editor Quentin Williams, Ryan Leary and Alex Webb for the outstanding review and suggestions.

References

An, Z., Kutzbach, J. E., Prell, W. L., & Porter, S. C. (2001). Evolution of Asian monsoons and phased uplift of the Himalaya–Tibetan plateau since Late Miocene times. *Nature*, *411*(6833), 62–66. https://doi.org/10.1038/35075035

Aydin, A., & Nur, A. (1982). Evolution of pull-apart basins and their scale independence. *Tectonics*, *1*(1), 91–105. https://doi.org/10.1029/TC001i001p00091

Cai, F. L., Ding, L., & Yue, Y. H. (2011). Provenance analysis of upper Cretaceous strata in the Tethys Himalaya, southern Tibet: Implications for timing of India-Asia collision. *Earth and Planetary Science Letters*, *305*(1–2), 195–206. https://doi.org/10.1016/j.epsl.2011.02.055

Chen, B. (2018). The discovery of thrust nappe structure in Qiashikansayi area on the northern margin of Altun Mountains and its tectonic significance. *Geological Bulletin of China*, *37*(2–3), 337–344.

Chen, L., Capitanio, F. A., Liu, L., & Gerya, T. V. (2017). Crustal rheology controls on the Tibetan plateau formation during India-Asia convergence. *Nature Communications*, *8*(1), 15992. https://doi.org/10.1038/ncomms15992

Chen, Z. L., Wang, X. F., Yin, A., Chen, B. L., & Chen, X. H. (2004). Cenozoic left-slip motion along the central Altyn Tagh Fault as inferred from the sedimentary record. *International Geology Review*, *46*(9), 839–856. https://doi.org/10.2747/0020-6814.46.9.839

Cheng, F., Guo, Z. J., Jenkins, H. S., Fu, S. T., & Cheng, X. (2015). Initial rupture and displacement on the Altyn Tagh fault, northern Tibetan Plateau: Constraints based on residual Mesozoic to Cenozoic strata in the western Qaidam Basin. *Geosphere*, *11*(3), 921–942. https://doi.org/10.1130/Ges01070.1

Cheng, F., Jolivet, M., Fu, S. T., Zhang, C. H., Zhang, Q. Q., & Guo, Z. J. (2016). Large-scale displacement along the Altyn Tagh Fault (North Tibet) since its Eocene initiation: Insight from detrital zircon U-Pb geochronology and subsurface data. *Tectonophysics*, *677*, 261–279. https://doi.org/10.1016/j.tecto.2016.04.023

Cheng, F., Jolivet, M., Hallot, E., Zhang, D. W., Zhang, C. H., & Guo, Z. J. (2017). Tectono-magmatic rejuvenation of the Qaidam craton, northern Tibet. *Gondwana Research*, *49*, 248–263. https://doi.org/10.1016/j.gr.2017.06.004

Cheng, F., Zuza, A. V., Haproff, P. J., Wu, C., Neudorf, C., Chang, H., et al. (2021). Accommodation of India-Asia convergence via strike-slip faulting and block rotation in the Qilian Shan fold-thrust belt, northern margin of the Tibetan Plateau. *Journal of the Geological Society*, *178*(3), jgs2020-207. https://doi.org/10.1144/jgs2020-207

Cheng, F., Zuza, A. V., Jolivet, M., Mulch, A., Meijer, N., & Guo, Z. (2023). Linking source and sink: The timing of deposition of Paleogene syntectonic strata in Central Asia. *Geology*, *51*(11), 1083–1088. https://doi.org/10.1130/g51382.1

Christie-Blick, N., & Biddle, K. T. (1985). Deformation and basin formation along strike-slip faults. In *Strike-slip deformation, basin formation, and sedimentation* (Vol. 37). SEPM Society for Sedimentary Geology.

Cowgill, E., Yin, A., Xiao Feng, W., & Qing, Z. (2000). Is the North Altyn fault part of a strike-slip duplex along the Altyn Tagh fault system? *Geology*, *28*(3), 255–258. https://doi.org/10.1130/0091-7613(2000)028<0255:Itnafp>2.3.Co;2

Dayem, K. E., Houseman, G. A., & Molnar, P. (2009). Localization of shear along a lithospheric strength discontinuity: Application of a continuous deformation model to the boundary between Tibet and the Tarim Basin. *Tectonics*, *28*(3), TC3002. https://doi.org/10.1029/2008tc002264

Ding, L., Kapp, P., Cai, F., Garzione, C. N., Xiong, Z., Wang, H., & Wang, C. (2022). Timing and mechanisms of Tibetan Plateau uplift. *Nature Reviews Earth & Environment*, *3*(10), 652–667. https://doi.org/10.1038/s43017-022-00318-4

Dupont-Nivet, G., Robinson, D., Butler, R. F., Yin, A., & Melosh, H. J. (2004). Concentration of crustal displacement along a weak Altyn Tagh fault: Evidence from paleomagnetism of the northern Tibetan Plateau. *Tectonics*, *23*(1), TC1020. https://doi.org/10.1029/2002tc001397

England, P., & Houseman, G. (1985). Role of lithospheric strength heterogeneities in the tectonics of Tibet and neighboring regions. *Nature*, *315*(6017), 297–301. https://doi.org/10.1038/315297a0

Gao, S. B., Cowgill, E., Wu, L., Lin, X. B., Cheng, X. G., Yang, R., et al. (2022). From left slip to transpression: Cenozoic tectonic evolution of the North Altyn Fault, NW margin of the Tibetan Plateau. *Tectonics*, *41*(3), e2021TC006962. https://doi.org/10.1029/2021TC006962

Green, P., & Duddy, I. (2021). Discussion: Extracting thermal history from low temperature thermochronology. A comment on recent exchanges between Vermeesch and Tian and Gallagher and Ketcham. *Earth-Science Reviews*, *216*, 103197. https://doi.org/10.1016/j.earscirev.2020.103197

He, P. J., Song, C. H., Wang, Y. D., Wang, D. C., Chen, L. H., Meng, Q. Q., & Fang, X. M. (2021). Early Cenozoic activated deformation in the Qilian Shan, northeastern Tibetan Plateau: Insights from detrital apatite fission-track analysis. *Basin Research*, *33*(3), 1731–1748. https://doi.org/10.1111/bre.12533

Hu, X., Wu, L., Zhang, Y., Zhang, J., Wang, C., Tang, J., et al. (2022). Multiscale lithospheric buckling dominates the Cenozoic subsidence and deformation of the Qaidam Basin: A new model for the growth of the northern Tibetan Plateau. *Earth-Science Reviews*, *234*, 104201. https://doi.org/10.1016/j.earscirev.2022.104201

Hu, X. M., Garzanti, E., Moore, T., & Raffi, I. (2015). Direct stratigraphic dating of India-Asia collision onset at the Selandian (middle Paleocene, 59 ± 1 Ma). *Geology*, *43*(10), 859–862. https://doi.org/10.1130/G36872.1

Huangfu, P., Li, Z.-H., Fan, W., Zhang, K.-J., & Shi, Y. (2022). Contrasting collision-induced far-field orogenesis controlled by thermo-rheological properties of the composite terrane. *Gondwana Research*, *103*, 404–423. https://doi.org/10.1016/j.gr.2021.10.020

Jiao, L., Tapponnier, P., Donzé, F. V., Scholtès, L., Gaudemer, Y., & Xu, X. (2023). Discrete element modeling of southeast Asia's 3D lithospheric deformation during the Indian collision. *Journal of Geophysical Research: Solid Earth*, *128*(1), e2022JB025578. https://doi.org/10.1029/2022jb025578

Jolivet, M., Brunel, M., Seward, D., Xu, Z., Yang, J., Roger, F., et al. (2001). Mesozoic and Cenozoic tectonics of the northern edge of the Tibetan plateau: Fission-track constraints. *Tectonophysics*, *343*(1–2), 111–134. https://doi.org/10.1016/S0040-1951(01)00196-2

Jolivet, M., Dominguez, S., Charreau, J., Chen, Y., Li, Y., & Wang, Q. (2010). Mesozoic and Cenozoic tectonic history of the central Chinese Tian Shan: Reactivated tectonic structures and active deformation. *Tectonics*, *29*(6), TC6019. https://doi.org/10.1029/2010tc002712

Kelly, S., Beaumont, C., & Butler, J. P. (2020). Inherited terrane properties explain enigmatic post-collisional Himalayan-Tibetan evolution. *Geology*, *48*(1), 8–14. https://doi.org/10.1130/G46701.1

Kong, X., Yin, A., & Harrison, T. M. (1997). Evaluating the role of preexisting weaknesses and topographic distributions in the Indo-Asian collision by use of a thin-shell numerical model. *Geology*, *25*(6), 527–530. https://doi.org/10.1130/0091-7613(1997)025<0527:Etropw>2.3.Co;2

Li, J. X., Yue, L. P., Roberts, A. P., Hirt, A. M., Pan, F., Guo, L., et al. (2018). Global cooling and enhanced Eocene Asian mid-latitude interior aridity. *Nature Communications*, *9*(1), 3026. https://doi.org/10.1038/s41467-018-05415-x

Lu, H. J., Ye, J. C., Guo, L. C., Pan, J. W., Xiong, S. F., & Li, H. B. (2019). Towards a clarification of the provenance of Cenozoic sediments in the northern Qaidam Basin. *Lithosphere*, *11*(2), 252–272. https://doi.org/10.1130/L1037.1

Mouthereau, F., Watts, A. B., & Burov, E. (2013). Structure of orogenic belts controlled by lithosphere age. *Nature Geoscience*, *6*(9), 785–789. https://doi.org/10.1038/ngeo1902

Parrish, J. T., Rasbury, E. T., Chan, M. A., & Hasiotis, S. T. (2019). Earliest Jurassic U-Pb ages from carbonate deposits in the Navajo Sandstone, southeastern Utah, USA. *Geology*, *47*(11), 1015–1019. https://doi.org/10.1130/G46338.1

Qi, B. S., Hu, D. G., Yang, X. X., Zhang, Y. L., Tan, C. X., Zhang, P., & Feng, C. J. (2016). Apatite fission track evidence for the Cretaceous-Cenozoic cooling history of the Qilian Shan (NW China) and for stepwise northeastward growth of the northeastern Tibetan Plateau since early Eocene. *Journal of Asian Earth Sciences*, *124*, 28–41. https://doi.org/10.1016/j.jseaes.2016.04.009

Qinghai Bureau of Geology and Mineral Resources (QBGMR). (1986). *Geologic Map of the Eboliang Sheet (scale 1:200,000)*. Geological Publishing House.

Rembe, J., Zhou, R., Sobel, E. R., Kley, J., Chen, J., Zhao, J.-X., et al. (2022). Calcite U–Pb dating of altered ancient oceanic crust in the North Pamir, Central Asia. *Geochronology*, *4*(1), 227–250. https://doi.org/10.5194/gchron-4-227-2022

Roberts, N. M. W., Drost, K., Horstwood, M. S. A., Condon, D. J., Chew, D., Drake, H., et al. (2020). Laser ablation inductively coupled plasma mass spectrometry (LA-ICP-MS) U–Pb carbonate geochronology: Strategies, progress, and limitations. *Geochronology*, *2*(1), 33–61. https://doi.org/10.5194/gchron-2-33-2020

Shi, W. B., Wang, F., Yang, L. K., Wu, L., & Zhang, W. B. (2018). Diachronous growth of the Altyn Tagh mountains: Constraints on propagation of the northern Tibetan margin from (U-Th)/He dating. *Journal of Geophysical Research-Solid Earth*, *123*(7), 6000–6018. https://doi.org/10.1029/2017jb014844

Sobel, E. R., Arnaud, N., Jolivet, M., Ritts, B. D., & Brunel, M. (2001). Jurassic to Cenozoic exhumation history of the Altyn Tagh range, northwest China, constrained by $^{40}Ar/^{39}Ar$ and apatite fission track thermochronology. In *Paleozoic and Mesozoic Tectonic Evolution of Central and Eastern Asia: From Continental Assembly to Intracontinental Deformation* (Vol. 194). Geological Society of America.

Tapponnier, P., Zhiqin, X., Roger, F., Meyer, B., Arnaud, N., Wittlinger, G., & Jingsui, Y. (2001). Oblique stepwise rise and growth of the Tibet plateau. *Science*, *294*(5547), 1671–1677. https://doi.org/10.1126/science.105978

Wang, E., Xu, F.-Y., Zhou, J.-X., Wang, S., Fan, C., Wang, G., et al. (2008). Vertical-axis bending of the Altyn Tagh belt along the Altyn Tagh fault: Evidence from late Cenozoic deformation within and around the Xorkol Basin. In *Investigations into the Tectonics of the Tibetan Plateau* (Vol. 444). Geological Society of America.

Wang, W., Zheng, W., Zhang, P., Li, Q., Kirby, E., Yuan, D., et al. (2017). Expansion of the Tibetan Plateau during the Neogene. *Nature Communications*, *8*(1), 15887. https://doi.org/10.1038/ncomms15887

Wu, L., Lin, X. B., Cowgill, E., Xiao, A. C., Cheng, X. G., Chen, H. L., et al. (2019). Middle Miocene reorganization of the Altyn Tagh fault system, northern Tibetan Plateau. *Geological Society of America Bulletin*, *131*(7–8), 1157–1178. https://doi.org/10.1130/B31875.1

Wu, S. T., Yang, Y. H., Roberts, N. M. W., Yang, M., Wang, H., Lan, Z. W., et al. (2022). In situ calcite U-Pb geochronology by high-sensitivity single-collector LA-SF-ICP-MS. *Science China Earth Sciences*, *65*(6), 1146–1160. https://doi.org/10.1007/s11430-021-9907-1

Xie, H., Liu, C., Zhang, H., Zhan, Y., & Zhao, X. (2022). Cenozoic evolution of the Altyn Tagh fault:Evidence from sedimentary records of basins along the fault. *Acta Petrologica Sinica*, *38*(4), 1107–1125. https://doi.org/10.18654/1000-0569/2022.04.09

Xie, R., Chen, L., Yin, A., Xiong, X., Chen, Y. J., Guo, Z., & Wang, K. (2023). Two phases of crustal shortening in northeastern Tibet as a result of a stronger Qaidam lithosphere during the Cenozoic India–Asia collision. *Tectonics*, *42*(1), e2022TC007261. https://doi.org/10.1029/2022tc007261

Xinjiang Bureau of Geology and Mineral Resources (XBGMR). (1981). *Geologic Map of the Xorkoli Sheet (scale 1:200,000)*. Geological Publishing House.

Xu, X., Zuza, A. V., Yin, A., Lin, X. B., Chen, H. L., & Yang, S. F. (2021). Permian plume-strengthened Tarim lithosphere controls the Cenozoic deformation pattern of the Himalayan-Tibetan orogen. *Geology*, *49*(1), 96–100. https://doi.org/10.1130/G47961.1

Yi, K., Cheng, F., Jolivet, M., Li, J., & Guo, Z. (2023). Supporting Information for 'Calcite U-Pb ages constrain Paleocene motion along the Altyn Tagh fault in response to the India-Asia collision'. Retrieved from https://figshare.com/s/2121ebd2938cf7236a11

Yin, A., & Harrison, T. M. (2000). Geologic evolution of the Himalayan-Tibetan orogen. *Annual Review of Earth and Planetary Sciences*, *28*(1), 211–280. https://doi.org/10.1146/annurev.earth.28.1.211

Yin, A., Rumelhart, P. E., Butler, R., Cowgill, E., Harrison, T. M., Foster, D. A., et al. (2002). Tectonic history of the Altyn Tagh fault system in northern Tibet inferred from Cenozoic sedimentation. *Geological Society of America Bulletin*, *114*(10), 1257–1295. https://doi.org/10.1130/0016-7606(2002)114<1257:Thotat>2.0.Co;2

Yue, Y. J., & Liou, J. G. (1999). Two-stage evolution model for the Altyn Tagh fault, China. *Geology*, *27*(3), 227–230. https://doi.org/10.1130/0091-7613(1999)027<0227:Tsemft>2.3.Co;2

Zuza, A. V., Gavillot, Y., Haproff, P. J., & Wu, C. (2020). Kinematic evolution of a continental collision: Constraining the Himalayan-Tibetan orogen via bulk strain rates. *Tectonophysics*, *797*, 228642. https://doi.org/10.1016/j.tecto.2020.228642

References From the Supporting Information

Bovet, P. M., Ritts, B. D., Gehrels, G., Abbink, A. O., Darby, B., & Hourigan, J. (2009). Evidence of Miocene crustal shortening in the north Qilian Shan from Cenozoic stratigraphy of the western Hexi Corridor, Gansu Province, China. *American Journal of Science*, *309*(4), 290–329. https://doi.org/10.2475/00.4009.02

Chen, Z. L., Gong, H. L., Li, L., Wang, X. F., Chen, B. L., & Chen, X. H. (2006). Cenozoic uplifting and exhumation process of the Altyn Tagh mountains. *Earth Science Frontiers*, *13*(4), 91–102.

Clark, M. K., Farley, K. A., Zheng, D. W., Wang, Z. C., & Duvall, A. R. (2010). Early Cenozoic faulting of the northern Tibetan Plateau margin from apatite (U-Th)/He ages. *Earth and Planetary Science Letters*, *296*(1–2), 78–88. https://doi.org/10.1016/j.epsl.2010.04.051

Duvall, A. R., Clark, M. K., Kirby, E., Farley, K. A., Craddock, W. H., Li, C. Y., & Yuan, D. Y. (2013). Low-temperature thermochronometry along the Kunlun and Haiyuan Faults, NE Tibetan Plateau: Evidence for kinematic change during late-stage orogenesis. *Tectonics*, *32*(5), 1190–1211. https://doi.org/10.1002/tect.20072

Fang, X. M., Zhang, W. L., Meng, Q. Q., Gao, J. P., Wang, X. M., King, J., et al. (2007). High-resolution magneto stratigraphy of the Neogene Huaitoutala section in the eastern Qaidam Basin on the NE Tibetan Plateau, Qinghai Province, China and its implication on tectonic uplift of the NE Tibetan Plateau. *Earth and Planetary Science Letters*, *258*(1–2), 293–306. https://doi.org/10.1016/j.epsl.2007.03.042

Gao, S. B., Cowgill, E., Wu, L., Lin, X. B., Cheng, X. G., Yang, R., et al. (2022). From left slip to transpression: Cenozoic tectonic evolution of the North Altyn Fault, NW margin of the Tibetan Plateau. *Tectonics*, *41*(3), e2021TC006962. https://doi.org/10.1029/2021TC006962

He, P. J., Song, C. H., Wang, Y. D., Chen, L. H., Chang, P. F., Wang, Q. Q., & Ren, B. (2017). Cenozoic exhumation in the Qilian Shan, northeastern Tibetan Plateau: Evidence from detrital fission track thermochronology in the Jiuquan Basin. *Journal of Geophysical Research-Solid Earth*, *122*(8), 6910–6927. https://doi.org/10.1002/2017jb014216

Hill, C. A., Polyak, V. J., Asmerom, Y., & Provencio, P. (2016). Constraints on a Late Cretaceous uplift, denudation, and incision of the Grand Canyon region, southwestern Colorado Plateau, USA, from U-Pb dating of lacustrine limestone. *Tectonics*, *35*(4), 896–906. https://doi.org/10.1002/2016tc004166

Ji, J. L., Zhang, K. X., Clift, P. D., Zhuang, G. S., Song, B. W., Ke, X., & Xu, Y. D. (2017). High-resolution magnetostratigraphic study of the Paleogene-Neogene strata in the Northern Qaidam Basin: Implications for the growth of the Northeastern Tibetan Plateau. *Gondwana Research*, *46*, 141–155. https://doi.org/10.1016/j.gr.2017.02.015

Jolivet, M., Roger, F., Arnaud, N., Brunel, M., Tapponnier, P., & Seward, D. (1999). Exhumation history of the Altun Shan with evidence for the timing of the subduction of the Tarim block beneath the Altyn Tagh system, North Tibet. *Comptes Rendus De L Academie Des Sciences Serie Ii Fascicule a-Sciences De La Terre Et Des Planetes*, *329*(10), 749–755. https://doi.org/10.1016/S1251-8050(00)88495-5

Li, M., Tang, L. J., & Yuan, W. M. (2015). Middle Miocene-Pliocene activities of the North Altyn fault system: Evidence from apatite fission track data. *Arabian Journal of Geosciences*, *8*(11), 9043–9054. https://doi.org/10.1007/s12517-015-1873-9

Lin, X., Zheng, D. W., Sun, J. M., Windley, B. F., Tian, Z. H., Gong, Z. J., & Jia, Y. Y. (2015). Detrital apatite fission track evidence for provenance change in the Subei Basin and implications for the tectonic uplift of the Danghe Nan Shan (NW China) since the mid-Miocene. *Journal of Asian Earth Sciences*, *111*, 302–311. https://doi.org/10.1016/j.jseaes.2015.07.007

Liu, D. L., Li, H. B., Sun, Z. M., Pan, J. W., Wang, M., Wang, H., & Chevalier, M.-L. (2017). AFT dating constrains the Cenozoic uplift of the Qimen Tagh Mountains, Northeast Tibetan Plateau, comparison with LA-ICPMS Zircon U-Pb ages. *Gondwana Research*, *41*, 438–450. https://doi.org/10.1016/j.gr.2015.10.008

Mock, C., Arnaud, N. O., & Cantagrel, J. M. (1999). An early unroofing in northeastern Tibet? Constraints from $^{40}Ar/^{39}Ar$ thermochronology on granitoids from the eastern Kunlun range (Qianghai, NW China). *Earth and Planetary Science Letters*, *171*(1), 107–122. https://doi.org/10.1016/S0012-821x(99)00133-8

Pang, J. Z., Yu, J. X., Zheng, D. W., Wang, W. T., Ma, Y., Wang, Y. Z., et al. (2019). Neogene expansion of the Qilian Shan, north Tibet: Implications for the dynamic evolution of the Tibetan Plateau. *Tectonics*, *38*(3), 1018–1032. https://doi.org/10.1029/2018tc005258

Paton, C., Hellstrom, J., Paul, B., Woodhead, J., & Hergt, J. (2011). Iolite: Freeware for the visualisation and processing of mass spectrometric data. *Journal of Analytical Atomic Spectrometry*, *26*(12), 2508–2518. https://doi.org/10.1039/c1ja10172b

Petrus, J. A., & Kamber, B. S. (2012). VizualAge: A novel approach to laser ablation ICP-MS U-Pb geochronology data reduction. *Geostandards and Geoanalytical Research*, *36*(3), 247–270. https://doi.org/10.1111/j.1751-908X.2012.00158.x

Ritts, B. D., Yue, Y. J., Graham, S. A., Sobel, E. R., Abbink, O. A., & Stockli, D. (2008). From sea level to high elevation in 15 million years: Uplift history of the northern Tibetan Plateau margin in the Altun Shan. *American Journal of Science*, *308*(5), 657–678. https://doi.org/10.2475/05.2008.01

Roberts, N. M. W., Rasbury, E. T., Parrish, R. R., Smith, C. J., Horstwood, M. S. A., & Condon, D. J. (2017). A calcite reference material for LA-ICP-MS U-Pb geochronology. *Geochemistry, Geophysics, Geosystems*, *18*(7), 2807–2814. https://doi.org/10.1002/2016gc006784

Sun, J. M., Zhu, R. X., & An, Z. S. (2005). Tectonic uplift in the northern Tibetan Plateau since 13.7 Ma ago inferred from molasse deposits along the Altyn Tagh Fault. *Earth and Planetary Science Letters*, *235*(3–4), 641–653. https://doi.org/10.1016/j.epsl.2005.04.034

Vermeesch, P. (2018). IsoplotR: A free and open toolbox for geochronology. *Geoscience Frontiers*, *9*(5), 1479–1493. https://doi.org/10.1016/j.gsf.2018.04.001

Wang, F., Shi, W. B., Zhang, W. B., Wu, L., Yang, L. K., Wang, Y. Z., & Zhu, R. X. (2017). Differential growth of the northern Tibetan margin: Evidence for oblique stepwise rise of the Tibetan Plateau. *Scientific Reports*, *7*(1), 41164. https://doi.org/10.1038/srep41164

Wang, X. M., Wang, B. Y., Qiu, Z. X., Xie, G. P., Xie, J. Y., Downs, W., et al. (2003). Danghe area (western Gansu, China) biostratigraphy and implications for depositional history and tectonics of northern Tibetan Plateau. *Earth and Planetary Science Letters*, *208*(3–4), 253–269. https://doi.org/10.1016/S0012-821x(03)00047-5

Wang, Y. D., Zheng, J. J., & Zheng, Y. W. (2018). Mesozoic-Cenozoic exhumation history of the Qimen Tagh Range, northeastern margins of the Tibetan Plateau: Evidence from apatite fission track analysis. *Gondwana Research*, *58*, 16–26. https://doi.org/10.1016/j.gr.2018.01.014

Woodhead, J. D., & Hergt, J. M. (2001). Strontium, neodymium and lead isotope analyses of NIST glass certified reference materials: SRM 610, 612, 614. *Geostandards and Geoanalytical Research*, *25*(2–3), 261–266. https://doi.org/10.1111/j.1751-908x.2001.tb00601.x

Wu, S., Yang, M., Yang, Y., Xie, L., Huang, C., Wang, H., & Yang, J. (2020). Improved in situ zircon U–Pb dating at high spatial resolution (5–16 μm) by laser ablation–single collector–sector field–ICP–MS using Jet sample and X skimmer cones. *International Journal of Mass Spectrometry*, *456*, 116394. https://doi.org/10.1016/j.ijms.2020.116394

Wu, S., Yang, Y., Jochum, K. P., Romer, R. L., Glodny, J., Savov, I. P., et al. (2021). Isotopic compositions (Li-B-Si-O-Mg-Sr-Nd-Hf-Pb) and $Fe^{2+}/\Sigma Fe$ ratios of three synthetic andesite glass reference materials (ARM-1, ARM-2, ARM-3). *Geostandards and Geoanalytical Research*, *45*(4), 719–745. https://doi.org/10.1111/ggr.12399

Xue, K., Junliang, J., Kexin, Z., Xiaohu, K., Bowen, S., & Chaowen, W. (2013). Magnetostratigraphy and anisotropy of magnetic susceptibility of the Lulehe Formation in the northeastern Qaidam Basin. *Acta Geologica Sinica - English Edition*, *87*(2), 576–587. https://doi.org/10.1111/1755-6724.12069

Yin, A., Dang, Y. Q., Wang, L. C., Jiang, W. M., Zhou, S. P., Chen, X. H., et al. (2008). Cenozoic tectonic evolution of Qaidam basin and its surrounding regions (Part 1): The southern Qilian Shan-Nan Shan thrust belt and northern Qaidam basin. *Geological Society of America Bulletin*, *120*(7–8), 813–846. https://doi.org/10.1130/B26180.1

Yu, J. X., Pang, J. Z., Wang, Y. Z., Zheng, D. W., Liu, C. C., Wang, W. T., et al. (2019). Mid-Miocene uplift of the northern Qilian Shan as a result of the northward growth of the northern Tibetan Plateau. *Geosphere*, *15*(2), 423–432. https://doi.org/10.1130/Ges01520.1

Yu, J. X., Zheng, D. W., Pang, J. Z., Wang, Y. Z., Fox, M., Vermeesch, P., et al. (2019). Miocene range growth along the Altyn Tagh Fault: Insights from apatite fission track and (U-Th)/He thermochronometry in the western Danghenan Shan, China. *Journal of Geophysical Research-Solid Earth*, *124*(8), 9433–9453. https://doi.org/10.1029/2019jb017570

Yuan, D. Y., Champagnac, J. D., Ge, W. P., Molnar, P., Zhang, P. Z., Zheng, W. J., et al. (2011). Late Quaternary right-lateral slip rates of faults adjacent to the lake Qinghai, northeastern margin of the Tibetan Plateau. *Geological Society of America Bulletin*, *123*(9–10), 2016–2030. https://doi.org/10.1130/B30315.1

Yuan, W. M., Dong, J. Q., Wang, S. C., & Carter, A. (2006). Apatite fission track evidence for Neogene uplift in the eastern Kunlun Mountains, northern Qinghai-Tibet Plateau, China. *Journal of Asian Earth Sciences*, *27*(6), 847–856. https://doi.org/10.1016/j.jseaes.2005.09.002

Zhang, W. (2006). *High-resolution Cenozoic magnetostratigraphy in the Qaidam Basin and the Uplift of Tibetan Plateau* (Ph. D. thesis). Lanzhou University. (in Chinese).

Zheng, D. W., Clark, M. K., Zhang, P. Z., Zheng, W. J., & Farley, K. A. (2010). Erosion, fault initiation and topographic growth of the North Qilian Shan (northern Tibetan Plateau). *Geosphere*, *6*(6), 937–941. https://doi.org/10.1130/Ges00523.1

Zhuang, G. S., Johnstone, S. A., Hourigan, J., Ritts, B., Robinson, A., & Sobel, E. R. (2018). Understanding the geologic evolution of Northern Tibetan Plateau with multiple thermochronometers. *Gondwana Research*, *58*, 195–210. https://doi.org/10.1016/j.gr.2018.02.014